A FINITE ELEMENT METHOD FOR THE HELMHOLTZ EQUATION IN AXIALLY SYMMETRIC PROBLEMS OF UNDERWATER ACOUSTICS: ERROR ESTIMATES AND NUMERICAL EXPERIMENTS

D. A. Mitsoudis[1,2], N. A. Kampanis[2], V. A. Dougalis[1,2]

Abstract— **We consider the Helmholtz equation in a cylindrical, axially symmetric fluid waveguide with variable bottom. We solve the problem by a finite element code in the interior of the waveguide, coupled with a discretization of the nonlocal DtN map on the outflow boundary. The resulting code is used to solve some model problems of low to medium frequency underwater sound propagation.**

I. Introduction

The numerical solution of the Helmholtz equation in a waveguide is a central problem in computational underwater acoustics since it provides accurate simulations of sound propagation and backscattering at any angle. As a result, various numerical and semi–analytical tecniques have been developed for this purpose, [6]. Frequently, the physical domain of interest is axially symmetric, and consists of one or more fluid layers over a bottom of variable topography. Away from a point harmonic source of frequency f Hz (assumed to be located at depth $z = z_s$, and range $r = 0$) the acoustic pressure field $p = p(z, r)$ satisfies Helmholtz's equation in cylindrical coordinates

$$\Delta p + k^2(z, r)\, p = 0, \tag{1}$$

where $k(z, r) = k_0 n(z, r)$, $k_0 = 2\pi f / c_0$ is a reference wave number associated with a reference sound speed c_0, and n is the index of refraction of the fluid medium. The p.d.e. (1) is supplemented with a source boundary condition for small r and an outgoing radiation condition as r increases, with the pressure–release surface condition $p(0, r) = 0$, a homogeneous Dirichlet or Neumann bottom condition $p = 0$ or $\dfrac{\partial p}{\partial \nu} = 0$ and, in general, with the usual transmission conditions across layer interfaces.

We solve this boundary–value problem using the standard Galerkin finite element method with continuous, piecewise linear functions defined on a triangulation of the domain Ω. The domain is truncated at some finite range value $r = R_2$, where we pose, as a nonlocal boundary condition, the DtN map of the field in the exterior of the waveguide, (assumed to be eventually range–independent), [3], [5], [8]. The basic finite element code FENL that we use in our computations in this note was described in detail in [7] (`http://oalib.saic.com/Other/fenl`), and also in the `fenl.html` file that can be found in the above site. We made several modifications in the code that now allow it to handle more general bottom boundary conditions and, mainly, to simulate sound waves produced by sources at higher frequencies than those used in the numerical experiments of [7].

In the next section we outline the basic features of the numerical method, describe a relevant error estimate in a simplified setting of the problem, and comment briefly on the various software packages to which we couple our basic finite element module. In Section III, we show the results of some numerical experiments that we performed with the code. Although the code can handle several fluid layers and range – and depth – dependent k, cf. [7], we shall restrict ourselves in this note in test problems with one layer and $k = k_0 =$ const., for simplicity.

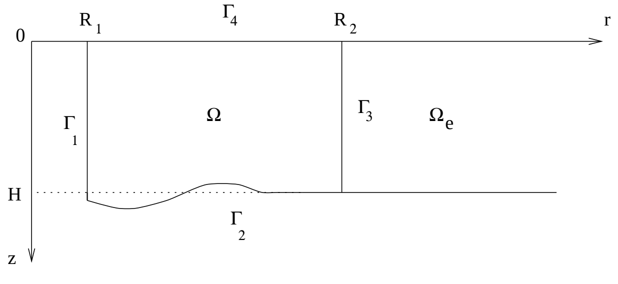

Fig. 1: Domain of the problem.

II. The finite element method

With reference to Figure 1, we consider the following boundary–value problem for (1), assuming that $k =$ const.. We seek a complex–valued function $p = p(z, r)$ defined in $\overline{\Omega}$ such that

$$p_{zz} + p_{rr} + \frac{1}{r} p_r + k^2 p = 0 \ \text{ in } \Omega, \tag{2}$$

$$p = g \ \text{ on } \Gamma_1, \tag{3}$$

$$\frac{\partial p}{\partial \nu} = 0 \text{ or } p = 0 \ \text{ on } \Gamma_2, \tag{4}$$

$$p = 0 \ \text{ on } \Gamma_4, \tag{5}$$

$$p_r = T(p) \ \text{ on } \Gamma_3. \tag{6}$$

[1]Department of Mathematics, University of Athens, 15784 Zographou, Greece
[2]Institute of Applied and Computational Mathematics, FO.R.T.H., 71110 Heraklion, Greece

Here $\frac{\partial p}{\partial \nu}$ is the normal derivative on Γ_2, g is a given function simulating the effect on Γ_1 of the point source, and T is the DtN map of the acoustic field in Ω_e posed on Γ_3 and given, cf. [3], [5], [8], by $(Tp)(z) = \sum_{n=0}^{\infty} c_n(p)\, w_n(z)$, where $c_n(p) = \sqrt{\lambda_n}(\sigma_n'/\sigma_n)(p(\cdot, R_2), w_n)$, $\sigma_n' = \frac{dH_0^{(1)}}{dr}(\sqrt{\lambda_n}R_2)$, $\sigma_n = H_0^{(1)}(\sqrt{\lambda_n}R_2)$, $(w, u) = \int_0^H w\overline{u}\, dz$, $H_0^{(1)}$ is the Hankel function of the first kind and zero order, and λ_n, $w_n(z)$, the eigenvalues and orthonormal eigenfunctions of the two–point depth eigenvalue problem $w'' + (k^2 - \lambda)w = 0$ in $[0, H]$, with $w(0) = 0$ and $w'(H) = 0$ or $w(H) = 0$, according to which boundary condition holds on Γ_2.

We discretize the boundary–value problem (2)–(6) using the standard Galerkin/finite element method with P_1 triangular elements of maximal side h. The nonlocal boundary condition (6) becomes a generalized natural boundary condition on Γ_3 and is approximated by a discrete analog evaluated as a finite sum including all the propagation and the most significant of the evanescent modes. We let p_h denote the approximation to (2)–(6) constructed in this manner.

The error estimate for this discretization proved by Goldstein, [5], for two–dimensional problems in Cartesian coordinates may be extended to the case of cylindrical coordinates for axisymmetric domains like those of Figure 1. In [9] it is proved (under the assumptions that the continuous problem (2)–(6) – with homogeneous Dirichlet boundary condition on Γ_2 – has a unique, sufficiently smooth solution, and for h sufficiently small), that the $L^2(\Omega)$ norm of the error $p - p_h$ is of $O(h^2)$ if we define $T(p)$ as above, i.e. take the infinite sum over the eigenfunctions. If the series is truncated so that the sum extends over all the propagating ($\lambda_n > 0$) and sufficiently many of the evanescent modes (for which $\lambda_n < 0$), one may prove e.g., cf. [5], [9], that the error bound in the $H^1(\Omega)$ norm of $p - p_h$ is of $O(h)$ plus a term which decays exponentially at the rate $-\frac{1}{2}\sqrt{-\lambda_J}(R_2 - R_1)$, where J is the order of the first evanescent mode that is ignored.

The basic finite element module is incorporated in the Fortran code FENL described in detail in [7]. The code uses mesh generation techniques from the MODULEF library, [1], appropriate preconditioned iterative solvers for indefinite, sparse, complex linear systems from the QMRPACK package, [4], routines from EISPACK for solving numerically the depth eigenvalue problem associated with T, and the PDE Toolbox of MATLAB for visualization of the computed field.

III. Numerical experiments

Test Problem 1. In a first experiment aimed to assess the accuracy of the method, we took as Ω the rectangle $0 < z < H$, $R_1 < r < R_2$ with zero Neumann boundary condition on Γ_2. We let the exact solution to (2)–(6) be given in this case by the function

$$p(z, r) = \sum_{n=1}^{M} H_0^{(1)}(\sqrt{\lambda_n}r)\, w_n(z),$$

where

$$\lambda_n = k^2 - \left[\frac{(2n-1)\pi}{2H}\right]^2, \; n = 1, \ldots, M,$$

and

$$w_n(z) = \sin\frac{(2n-1)\pi z}{2H}, \; n = 1, \ldots, M,$$

where M is the number of the propagating modes, i.e. satisfies, for a given k, $\lambda_M > 0 > \lambda_{M+1}$. (We took $g(z) = p(z, R_1)$, $0 \le z \le H$). We solved the problem numerically on a uniform triangulation with isosceles right triangles of perpendicular side h_w, using as a linear solver the routine QMR of QMRPACK with the two–sided ILUT preconditioner, [4]. We let $\xi = c/(fh_w)$ be the number of meshlengths per wavelength, $c = 1500$ m/sec and $H = 50$ m, and ran a series of cases summarized in the table below. In each case the length $R_2 - R_1$ of the domain contains about five wavelengths. For each run we indicate the value of the parameters f, M, R_1, R_2, the number N of finite elements, the values of h_w and ξ, and the value of the normalized l^2 error defined as $(\sum |p_h(Q) - p(Q)|^2 / \sum |p(Q)|^2)^{1/2}$ where the sum is taken over all the nodes Q of the triangulation. (The units are Hz for f and meters for all lengths.)

f	M	R_1	R_2	N	h_w	ξ	ε
15	1	100	600	4500	3.333	30	0.0159
15	1	100	600	12500	2.0	50	0.0060
15	1	100	600	50000	1.0	100	0.0015
45	3	35	185	33750	0.666	50	0.0096
45	3	35	185	54150	0.526	63.3	0.0060
75	5	20	120	40000	0.5	40	0.0192
90	6	20	120	40000	0.5	33.3	0.0349

From this table and other data not shown here one can confirm that for a fixed frequency f the error is of $O(h^2)$. In addition, we observe that at the frequency $f = 15$ Hz, in order to achieve an error of 10^{-2} we need to take at least $\xi = 39$, while for an error of $5 \cdot 10^{-2}$ we need $\xi = 55$. At $f = 45$ Hz one may take $\xi = 49$ and 69, respectively. In Figure 2 we show the superimposed moduli of the exact and the approximate solution as functions of r for the $f = 45$ Hz run with 33750 elements at a depth of 30 m, while in Figure 3 we show the analogous graph for the run with $f = 90$ Hz at a depth of 30 m as well. We conclude that the code can simulate accurately solutions of the Helmholtz equation in small–to–middle scale problems. The most time consuming run was the $f = 90$ Hz one, which took 504 CPU secs on a Pentium III PC with a RAM of 128 MB running under Linux at 550 MHz. For this run we used the QMRPACK QMR routine with a two–sided ILUT preconditioner with parameters fill–in=2 and tolerance=10^{-3}; the solver required 521 iterations to converge.

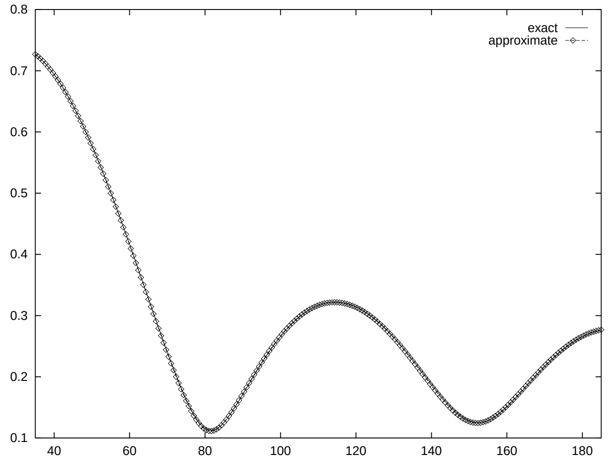

Fig. 2: Test Problem 1, f=45 Hz, z=30 m

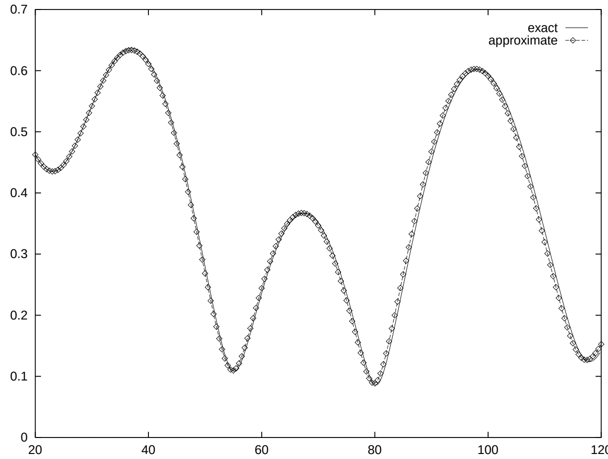

Fig. 3: Test Problem 1, f=90 Hz, z=30 m

Test Problem 2. In a second test problem (Figures 4, 5, 6) we considered a domain consisting of water with c = 1500 m/sec of depth 50 m and R_1 = 100 m, R_2 = 600 m with an (axisymmetric) step on the bottom of height 5 m extending from $r = 200$ to $r = 400$ m. We took as effective source on Γ_1 the function $g(z) = \sqrt{\frac{k}{2}}[\exp(-\frac{k^2}{4}(z-z_s)^2) - \exp(-\frac{k^2}{4}(z+z_s)^2)]$ with z_s = 10 m, and a homogeneous Neumann b.c. on all five segments of the bottom curve. In Figures 4, 5, 6 the number of finite elements used was $N = 48000$. Figure 4 shows the modulus of the pressure field generated when f = 15 Hz. (The form of the field is practically the same with that generated by a source function from the widely used normal mode code COUPLE [2]; as was verified in [7] (Test Case 6), the FENL results are in good agreement with the results of COUPLE for this problem). In Figure 4 $M = 1$ mode propagates and ξ was equal to 100 meshlengths/wavelength. In Figure 5 we raised the frequency to f = 30 Hz and took $\xi = 50$. Now $M = 2$ modes propagate. Finally, in Figure 6 f was 45 Hz, 3 modes propagate and $\xi = 33$.

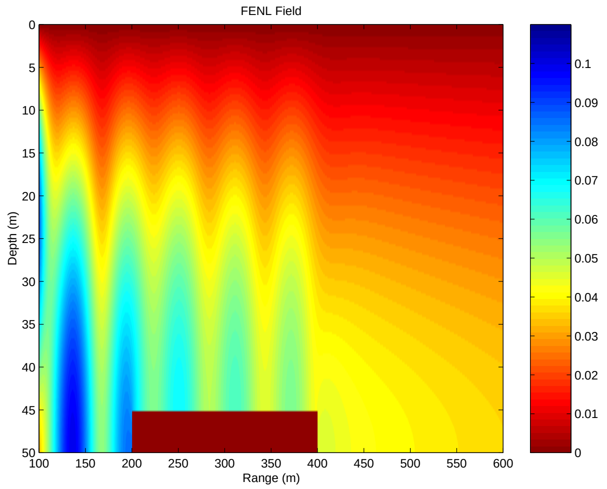

Fig. 4: Test Problem 2, f=15 Hz

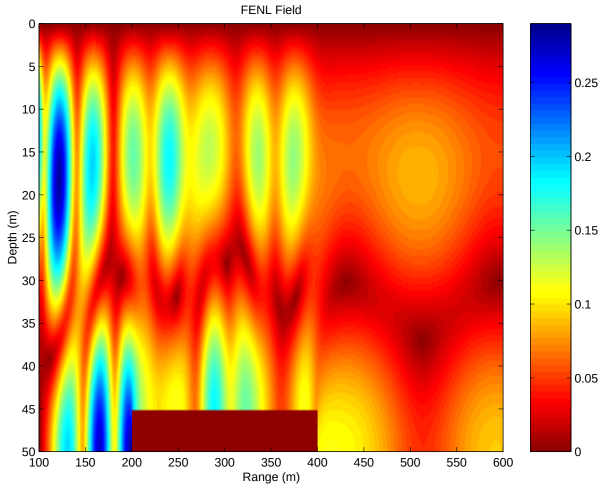

Fig. 5: Test Problem 2, f=30 Hz

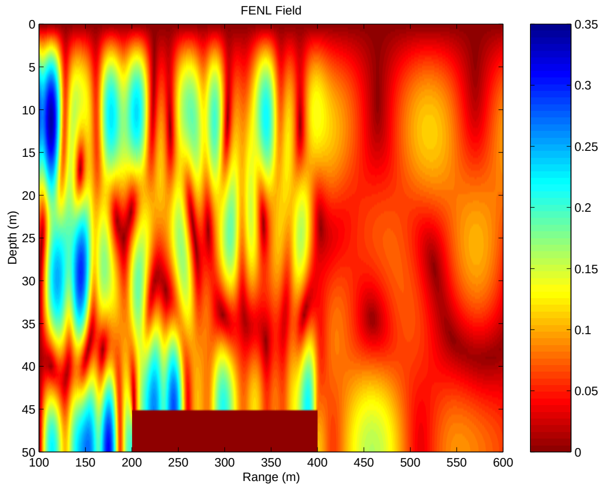

Fig. 6: Test Problem 2, f=45 Hz

Test Problem 3. In a third test problem (Figures 7 – 10) we took a rectangular domain of depth 50 m and $[R_1, R_2]$=[10m,110m], consisting of water with c = 1500 m/sec. We took the same source function as in Test Problem 2 at a frequency f = 85 Hz. A homogeneous Dirichlet b.c. was imposed in the bottom. Figure 7 shows the computed modulus of the pressure field for this problem with 40000 elements, $\xi = 35$ and 5 propagating modes; the wavelength of the sound field was $\lambda = 17.65$ m. Figures 8, 9 and 10 show the distortions of the field brought upon by the presence of an (axisymmetric) hard circular disk (i.e. an impermeable ring–type structure with a zero Neumann boundary condition on its surface), having diameter $\delta =$ 20m, 10m and 4m, respectively.

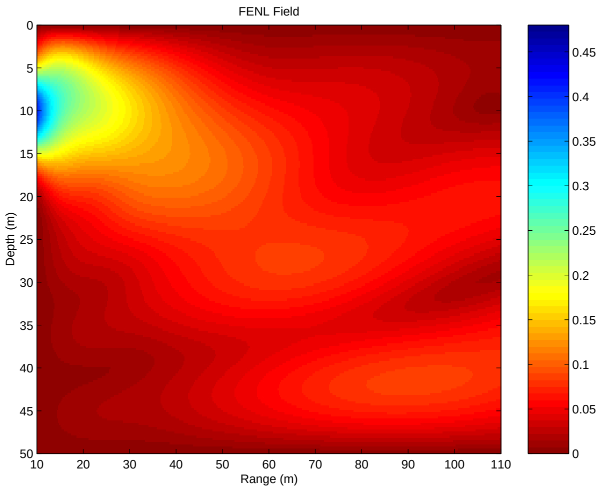

Fig. 7: Test Problem 3, no obstacle

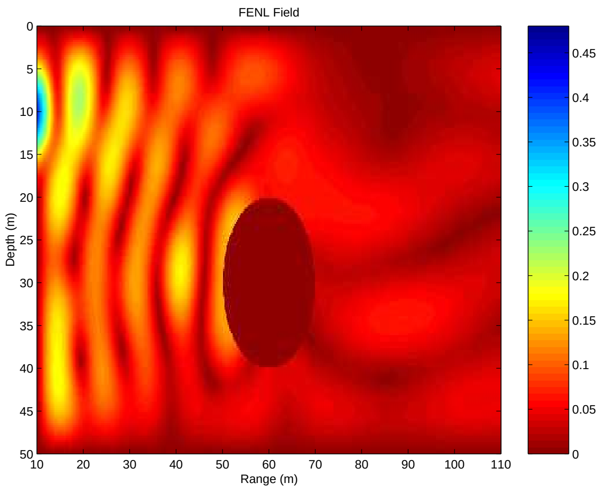

Fig. 8: Test Problem 3, δ=20m

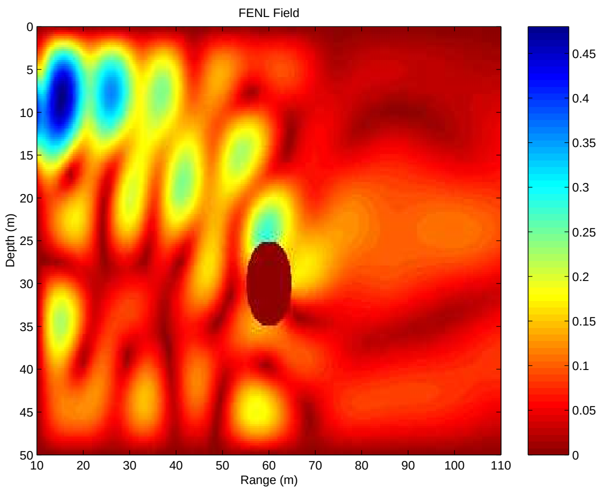

Fig. 8: Test Problem 3, δ=10m

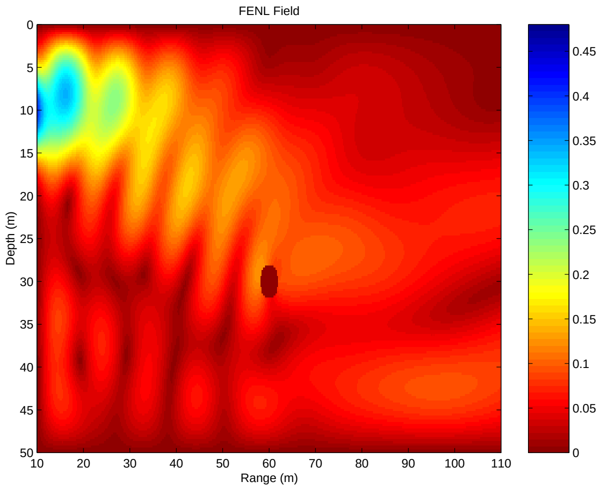

Fig. 10: Test Problem 3, δ=4m

This experiment gives some idea of the sensitivity of the computed field to obstacles near the source.

Acknowledgments

This work was supported in part by the Institute of the Applied and Computational Mathematics of FO.R.T.H., and in part by a grant by the Research Committee of the University of Athens.

References

[1] M. Bernadou, P. L. George, A. Hassim, P. Joly, P. Laug, A. Perronnet, E. Saltel, D. Steer, G. Vanderborck and M. Vidrascu, *MODULEF: A Modular Library of Finite Elements*, INRIA, 1988.

[2] R. B. Evans, "COUPLE: A user's manual", NORDA TN–332 (1986).

[3] G. J. Fix, S. P. Marin, "Variational methods for underwater acoustic problems", *J. Comp. Physics* **28** (1978), 253–270.

[4] R. W. Freund, N. M. Nachtigal, "An implementation of the QMR method based on coupled two–term recurrences", *SIAM J. Sci. Comput.* **15** (1994), 313–337.

[5] C. I. Goldstein, "A finite element method for solving Helmholtz type equations in waveguides and other unbounded domains", *Math. Comp.* **39** (1982), 309–324.

[6] F. B. Jensen, W. A. Kuperman, M. B. Porter and H. Schmidt, *Computational Ocean Acoustics*, American Institute of Physics, New York, 1993.

[7] N. A. Kampanis, V. A. Dougalis, "A finite element code for the numerical solution of the Helmholtz equation in axially symmetric waveguides with interfaces", *J. Comp. Acoustics* **7** (1999), 83–110.

[8] J. B. Keller, D. Givoli, "Exact nonreflecting boundary conditions", *J. Comp. Physics* **82** (1989), 172–192.

[9] D. A. Mitsoudis, "Finite element methods for time–harmonic wave propagation problems in underwater acoustics", Ph.D. Thesis, University of Athens, Greece (under preparation).